

# Sensitivity of Hydration Heat to Autogenous Shrinkage in Full-Scale High-Performance Concrete Beams

Hasti Riakara Husni<sup>1</sup>, Chatarina Niken<sup>2\*</sup> (Corresponding author)

<sup>1,2</sup>Civil Engineering Department, Faculty of Engineering, University of Lampung

Sumantri Brojonegoro Street No 1, Bandar Lampung, Indonesia

<sup>2\*</sup> E-mail of the corresponding author: chatarinaniken@yahoo.com

## Abstract

High-performance concrete is more susceptible to cracking at an early age. During hydration, various forces come into play, including heat generated by hydration, forces driving the growth of hydration products, and forces contributing to the reduction of pore number and size. Heat hydration is one of the things highlighted as the cause. The investigation of full-scale beam hydration heat aims to address the challenge of producing crack-free HPC. This research was carried out experimentally on full-scale prestressed beams measuring 200×600×3000 (mm) with a compressive strength ( $f_c'$ ) of 60 MPa. Shrinkage and temperature in the concrete were measured using vibrating wire-embedded strain gauges. Four gauges were installed at 1030 mm from each end, and another four were placed in the middle of the beam. After casting, the beam were immediately covered with burlap sacks to keep them consistently moist. Strain and temperature observations were recorded every 15 minutes starting immediately after casting. Eight autogenous shrinkage phenomena were identified in full-scale beams. Phenomena 1 and 6 showed no sensitivity to hydration heat release. Phenomenon 1 occurred within the first 3 hours, during which the surrounding temperature still influenced the concrete temperature. Phenomenon 6 took place at 20.5-20.7 hours, indicating a sudden jump in autogenous shrinkage not accompanied by heat of hydration. The critical period, from age 9.5 to 16 hours, sees the highest values of temperature and shrinkage in the concrete. At this time the beams can be given special treatment. A growth sketch of the hydration product has been proposed.

**Keywords:** Autogenous shrinkage, Beam, Concrete, Hydration heat

**DOI:** 10.7176/CER/15-3-06

**Publication date:** December 31<sup>st</sup> 2023

## 1. Introduction

Concrete beams are responsible for carrying the plate load, where the plate supports dead and live loads. Precast concrete beam with steam curing have been studied. The highest temperature reached 68.5°C at 14 hours (Cai *et al.* 2023). To withstand heavy loads or long spans, high-performance concrete (HPC) is an option. High-performance concrete is concrete that has an elastic modulus of 30~55 GPa or  $f_c'$  40~113MPa), and the drying shrinkage rate should be less than 0.04% to ensure its volume stability (Xu *et al.* 2021). The ability to resist shrinkage is the basis for determining the quality of concrete. Autogenous shrinkage of laboratory scale HPC is ±225 times the shrinkage of normal concrete with Portland composite cement (PCC) (Niken *et al.* 2023). Therefore, HPC is more susceptible to premature cracking.

The heat of hydration is the suspected cause of premature cracking in HPC. To mitigate this, researchers have explored various materials. These include the use of the pipe cooling method (Zhang *et al.* 2023), low heat cement (Jadhav 2021), microcapsules sustain release (MSR) as a sustained-release type hydration heat inhibitor (Jia *et al.* 2021), reducing the amount of cement, selecting coarse aggregates with larger particle sizes and high thermal expansion coefficients (Zhao *et al.* 2021), and using ground granulated blast furnace slag (GGBS) (Yalçınkaya *et al.* 2021) to reduce the heat of hydration.

The long-term performance of concrete is determined by its ability to withstand all forces since the hydration process occurs. During the hydration process, there is a heat force due to hydration, a force for the growth of hydration products, and a force for decreasing the number and size of pores. The hydration reaction is always followed by deformation. Deformation at an early age includes autogenous shrinkage because autogenous shrinkage is a change in volume due to the chemical process of cement hydration, not including the influence of applied loads and surrounding condition (ACI 209R 1992).

Changes in deformation from expansion to shrinkage and vice versa at an early age can occur quickly. The durability of the concrete in resisting these changes must also be met to prevent premature cracking. This happens intensely in the first 24 hours of concrete. If the concrete is not able to withstand all these forces, premature cracks will occur. So apart from concrete being required to be able to withstand the heat of hydration, it is also required to have the ability to produce hydration products such as CSH and CH which grow quickly, have good quality, and are elastic so that all forces and changes in volume can be withstood. The growth mechanisms of CSH and CH (portlandite) have been studied. Both can grow from the same place but the growth of portlandite crystals is inhibited by silicate ions (John & Lothenbach 2023).

The heat of hydration is influenced by the type of mix and the size of the concrete. Some researchers have studied autogenous shrinkage for mass concrete (Kim *et al.* 2009), and dams (Zhao *et al.* 2021; Kim 2010), but not many have studied it for full-scale beam. There is a close relationship between heat of hydration and autogenous shrinkage at an early age, especially between HHV (hydration heating rate) and ASV (autogenous shrinkage rate). The higher the HHV, the higher the ASV, and the greater the autogenous shrinkage. Thermal deformation is calculated using the thermal expansion coefficient (TEC) corrected by the maturity method, and subtracted from the total measured deformation (Kim *et al.* 2009).

It is a challenge to make high-strength concrete that is resistant to cracking and to explore the autogenous shrinkage of full-scale high-performance concrete beam and its sensitivity to the hydration temperature within them.

## 2. Materials and Methods

This research was carried out experimentally using one full-scale beam specimen measuring 200×600×3000 (mm) which was also prepared to be prestressed to depict the actual structure (Figure 1). The mold is covered with a thin sheet of plastic to prevent water absorption. The high-performance concrete used in the study has a strength of 60 MPa.

The material used in this research is coarse aggregate from crushed stone originating from Banten, West Java, Indonesia. The coarse aggregate consists of 70% with a size of 13-19 mm, specific gravity in the SSD (saturated surface-dry) state of 2.563, absorption of 1.543%, and 30% with a size of 6-12 mm, specific gravity in the SSD state of 2.636, and absorption of 2.26%. The fine aggregate is from Sungai Liat, Bangka, Sumatra, Indonesia, with a specific gravity under SSD conditions of 2.603 and an absorption of 0.4%. Other materials include ordinary Portland cement (OPC) produced by Indocement, Indonesia; silica fume; and high-range water reducer (HRWR) Viscocrete 10 produced by Sika Indonesia. Concrete mix proportions are presented in Table 1.

Tabel 1. Mix design

Material	Weight kg/m <sup>3</sup>
OPC	500
Silica fume	40
Coarse aggregate	935
Fine aggregate	800
HRWR	7.6
Water	142.6

The weight of fine aggregate and coarse aggregate in the SSD state is determined. Mixing is carried out using a mixing machine with a capacity of 0.3 cubic meters. The process begins by mixing the cementitious material in a dry state, followed by the addition of 50% fine aggregate and 50% water. The machine is then rotated for approximately 1.5 minutes. Subsequently, 50% of the water, already mixed with the high-range water reducer (HRWR), is added. The machine continues to rotate for approximately 3 minutes after a visible change in the flow of the remaining fine and coarse aggregates.

Maximum reinforcement, as shown in Figure 1, is used to accommodate heavy structures where maximum reinforcement is required. The detected heat means that it includes the influence of the reinforcement in it.

Deformation was measured as changes in strain over time by installing four vibrating wire-embedded strain gauges (VWESG) of Geokon type 4200 at the ends of the specimen and four in the middle of the specimen. The VWESG on the top layer is installed just before casting (Figure 2). VWESG can detect strains up to 3000  $\mu\epsilon$

with an accuracy of .025% and can measure temperatures in concrete between -80°C and 60°C with an accuracy of around 0.5%. Strain is calculated using Equation 1.

$$\Delta\mu\varepsilon = \frac{(R_1 - R_0)B}{Geokon} \quad (1)$$

Where:

$\Delta\mu\varepsilon$  : is the apparent change in microstrain

$R_0$  : is the initial reading in microstrain

$R_1$  : is a subsequent reading

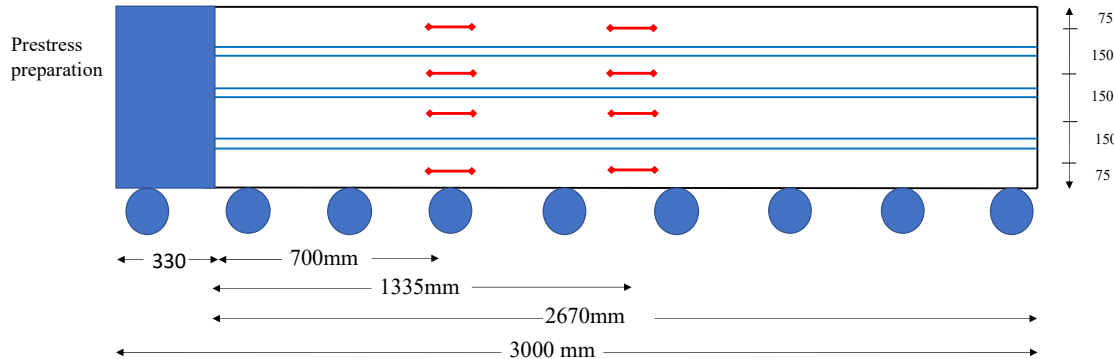


Figure 1. Reinforcement and VWESG installation scheme

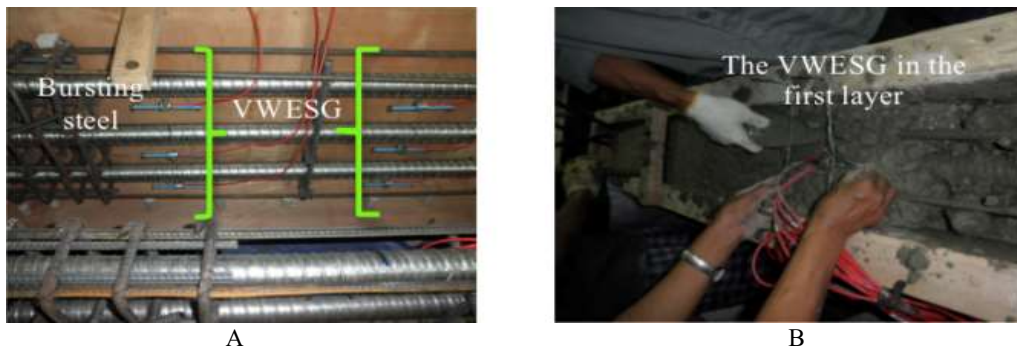


Figure 2. A: Placement of reinforcement and VWESG, B: Casting

The shear force between the specimen and the floor is eliminated by installing rollers at intervals of  $\pm 500$  mm, allowing the deflection caused by its weight to be eliminated (Figure 1). Observations were conducted by reading the output immediately after casting until the age of 24 hours at 15-minute intervals. The data from eight VWESGs, calculated based on Equation 1, are averaged to represent the strain of the specimen. This is done because the concrete behavior of each layer cannot be considered the same due to its position.

### 3. Result and Discussion

#### 3.1. Result

The results of the research in the form of deformation and temperature in the concrete are presented in Figure 3.

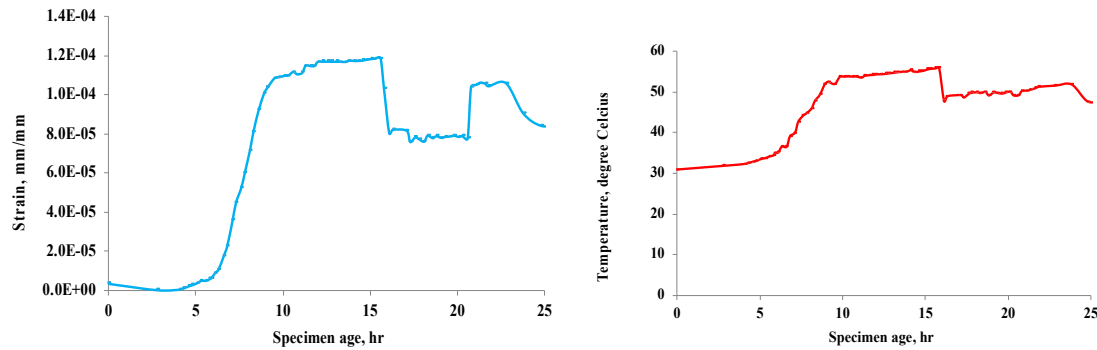


Figure 3. A: Concrete strain, B: Temperature inside the concrete

### 3.2. Discussion

The discussion initiates with an exploration of the material, as it significantly influences both shrinkage and hydration heat. Subsequently, the sensitivity of deformation to the hydration heat of concrete is addressed.

#### 3.2.1. Material

The hydration reaction and the quality of the hydration products are highly dependent on the chemical composition of the concrete, the quantity, and the treatment applied to it. The content of chemical elements in concrete is presented in Table 2.

Table 2. Chemical element in the specimen

Chemical element	In specimen, %	Chemical element	In specimen, %
MgO	0.9	CaO	67.16
Al <sub>2</sub> O <sub>3</sub>	3.45	TiO <sub>2</sub>	0.35
SiO <sub>2</sub>	19.89	MnO <sub>2</sub>	
P <sub>2</sub> O <sub>5</sub>	0.25	Fe <sub>2</sub> O <sub>3</sub>	5.3
S	1.36	CuO	0.09
K <sub>2</sub> O	1.18	ZnO	0.08

C<sub>3</sub>S, C<sub>2</sub>S, C<sub>3</sub>A and C<sub>4</sub>AF can be obtained by Equation 2-5 (SNI 15-2049 2004).

$$C_3S = (4.071 CaO - 7.6 SiO_2 - 6.718 Al_2O_3 - 1.43 Fe_2O_3 - 2.852 SO_3) \quad (2)$$

$$C_2S = -(2.867 SiO_2 - 0.7544 C_3S) \quad (3)$$

$$C_3A = 2.65 Al_2O_3 - 1.692 F_2O_3 \quad (4)$$

$$C_4AF = 3.043 Fe_2O_3 \quad (5)$$

From the data in Table 2 and Equations 2-5, values are obtained

$$C_3S = 91.5; C_2S = 12; C_3A = 0.17 \text{ and } C_4AF = 10.5$$

To achieve 80% reaction with water takes time:

C<sub>3</sub>S: ±10 days, C<sub>2</sub>S: ±100 days, C<sub>3</sub>A+H: ±6 days, C<sub>4</sub>AF + H: ±50 days, C<sub>3</sub>A + H + C: ±1 day (Irma *et al.* 2017).

For 24 hours, C<sub>3</sub>A + H + C has reached 80% of the reaction presented in Equation 6.



C<sub>3</sub>A 3CS H<sub>30-32</sub> (trisulfat or ettringite) (Irma *et al.* 2017).

With the same amount of each compound making up the cement, the heat rate of hydration is C<sub>3</sub>A (865 J/gm) > C<sub>3</sub>S (865 J/gm) > C<sub>3</sub>AF (420 J/gm) > C<sub>2</sub>S (260 J/gm) (Chhapola 2023)

The hydration product that determines the mechanical and volumetric properties of cement paste is calcium silicate aluminate hydrate (C(-A)-S-H) (Wang *et al.* 2022). The quality of CSH is contingent upon the water-to-cement (w/c) ratio and the calcium-to-silica (Ca/Si) ratio.

From Table 2 above, the Ca/Si value is 3.3, which is relatively high due to the Ca content because in Ordinary Portland Cement (OPC) being around 62%. The primary material for OPC is sourced from nearby limestone. It is noted that as the Ca/Si ratio increases, the compressive strength of the paste tends to decrease (Kunther *et al.* 2017). This mixture uses 8% silica fume or 2% below the maximum limit so that the destruction is not brittle (Yogendran *et al.* 1987). Even though the Ca and Ca/Si is high, the compressive strength of the concrete reaches 60 MPa at 28 days. Thus the selection of the amount of material is appropriate.

The mixture in this study adheres to ACI 211.4R with modifications, limiting the cement content to 500 kg/cubic m to approach a shrinkage ratio of 1 according to ACI 209R. The cement used is the OPC type. The concrete mixture is designed to have a flow slump of  $300 \pm 50$  mm, with a water-to-cementitious ratio of 0.26 to maintain the quality of CSH (Terkhajornkit & Nawa 2006).

### 3.2.1. Sensitivity of Autogenous Shrinkage to Hydration Heat

When water is added to cement, heat is released, with the rate and amount dependent on the cement composition. The heat of complete hydration is determined from the four main compounds of Portland cement:  $3\text{CaO} \cdot \text{SiO}_2$ ,  $2\text{CaO} \cdot \text{SiO}_2$ ,  $3\text{CaO} \cdot \text{Al}_2\text{O}_3$ , and  $4\text{CaO} \cdot \text{Al}_2\text{O}_3 \cdot \text{Fe}_2\text{O}_3$  (Lerch & Bogue, 1934). John and Lothenbach (2023) extensively reviewed the hydration mechanism from the late 19th century to 2023, concluding that the  $\text{C}_3\text{S}$  hydration reaction is controlled by dissolution and precipitation reactions leading to saturation. All reactions, including deformation and heat of hydration, are interconnected.

Finding the sensitivity of hydration heat to concrete strain is assisted by combining concrete behavior and changes in hydration heat as in Figure 4

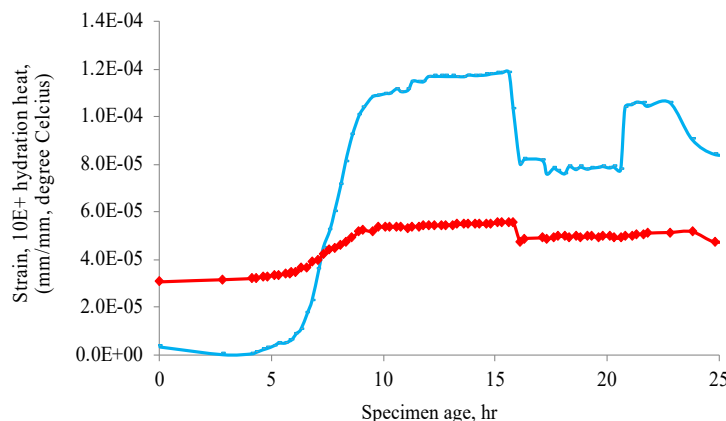


Figure 4. Concrete behavior and hydration heat

Changes in deformation behavior indicate the existence of certain phenomena within the beam. Detailed discussion of each phenomenon.

#### 3.2.1.1. Phenomenon 1

Between 1 – 3 hours, the concrete experiences expansion. Ten minutes after the concrete was mixed with water, ettringite grains were formed (Taylor 1997). The formation of ettringite is followed by expansion (Kurtis 2015). Alite ( $\text{C}_3\text{S}$ ) hydration, constituting 50-80% OPC, significantly contributes to concrete property evolution (Kumar *et al.* 2012). The alite hydration reaction produces  $\text{Ca}^{2+}$ . The growth of  $\text{Ca}^{2+}$  makes the volume expand. Maximum  $\text{Ca}^{2+}$  occurs 1 hour after hydration (Paulini 1990). From the discussion about materials in sub-chapter 3.2.1, it can be said that Ca dominance occurs gradually so that the top of the concrete expands to its maximum at 3 hours. (Figure 4). The heat of hydration immediately after casting reached  $30^\circ\text{C}$ , slightly higher than the air temperature at that time ( $29.5^\circ\text{C}$ ).

Concrete strain appears insensitive to internal hydration heat changes.

### 3.2.1.2. Phenomenon 2

After 3 hours of age, CSH begins to form. At first, the rate of formation is low then starting at 6 hours the rate of formation of CSH, CH is fast (Kurtis 2015). This aligns with the shrinkage rate in Figure 4.

The heat of hydration aged 6 – 9.5 hours increases at a high rate and reaches a maximum at the same age when maximum shrinkage occurs. C<sub>3</sub>S is the chemical content of concrete that reacts most quickly and emits high heat of hydration (Jadhav 2021). The C<sub>3</sub>S reaction produces CSH and CH emitting high heat. The temperature increase rate is 1.9°C/hour while the decrease rate is 7.6E-06/hour.

Concrete strain appears quite sensitive to internal temperature changes.

### 3.2.1.3. Phenomenon 3

The heat of hydration at 9.5-15.5 hours has a similar shape to the shrinkage. In this study, the highest concrete temperature is 55.9°C at 15.5 hours, with a maximum strain of 1.2E-04 (Figure 4).

Zhao *et al.* (2021) examined the dam and reported that the highest temperature was 49.4°C. Hydration heat flow at 24 hours was 2.4 kJ/kg-h, and the highest was 3.2 kJ/kg-h occurred at 30 hours. The cumulative heat release at 24 hours of cement paste w/b 0.3 is ±23 kJ/kg, and at 30 hours the value is 48 kJ/kg. Volumetric shrinkage at 24 hours is 3.25%, and at 30 hours is 3.6% (Hu *et al.* 2017). The specific heat capacity of concrete is 880 J/kg°C. Gravitational potential energy Q is presented in Equation 7 (Building Design).

$$Q = T \cdot \text{specific heat capacity} \quad (7)$$

By using Equation 7, the gravitational potential energy in this research Q = 49.192 J is obtained. This means that if at the highest shrinkage, the concrete does not crack, the concrete can withstand 49.192 N and lift particles as far as 1 m or to shift particles 1 millimeter it requires ±5 kilograms of force. With a mixture like Table 1, it is proven that the concrete bond can withstand this energy without cracking.

From 9.5 to 15.5 hours, the strain increases very slowly or can be said to be stable. In this period, ettringite and expansion by hydration reactions that occur under pressure are balanced by shrinkage by CSH and CH so that the strain becomes constant.

Concrete strain appears quite sensitive to internal temperature changes.

### 3.2.1.4. Phenomenon 4

Ettringite growth in normal concrete increases rapidly from 6 hours to 1 day, declining at 2-7 days. In this period the number of pores decreases at a moderate rate (Kurtis 2015). Meanwhile, in the study at 15.5-16.5 hours, the temperature falls by ±8°C and rises of strain by 4E-05 in 1 hour. The expansion force of ettringite exceeds the shrinkage force for ±1 hour due to the growth of hydration products and pore reduction. The reduction in the number of pores occurs because the pores are filled with hydration products, during this time, pore water is forced out of the pores and causes a decrease in temperature in the concrete.

In this period the strain pattern is similar to the temperature pattern in the concrete, so the concrete strain is quite sensitive to changes in internal temperature.

### 3.2.1.5. Phenomenon 5

Between 16.5 and 20.5 hours, there is a period where both the strain and temperature within the concrete remain constant. The growth pattern of ettringite in normal concrete (NC) occurring from 15 hours to 2 days (Kurtis 2015). Notably, the growth period for ettringite in this study was only 4 hours, whereas in normal concrete it occurs for 33 hours.

HPC can only be made with very limited water. Ettringite grows maximum at a more mature age than NC, creating a stronger bond. However, the elastic period of HPC is brief, posing a higher risk of premature cracking.

The causes of stable strain and temperature indicate that the behavior of concrete in this period is determined more by the balance between expansion forces and shrinkage forces. The compressive force that occurs during the hydration reaction causes the concrete to expand (Niken *et al.* 2017). The hydration reaction in this period is

very intensive because the growth of CSH and CH occurs at a high rate and this occurs under pressure by its weight for VWESH in the middle and lower parts, enhancing the expansive force within the concrete. This force is balanced by shrinkage due to the growth of CSH, CH and a decrease in the number of pores. Some pores contain water. The behavior of expanding and compressing by its weight makes the water in the pores come out which causes a decrease in temperature. However, this effect is balanced by the heat generated from the growth of hydration products, resulting in a stagnant internal temperature. This distinction highlights the divergence between the behaviors of laboratory-scale and full-scale concrete.

So concrete strain is revealed to be sensitive to changes in temperature.

#### 3.2.1.6. Phenomenon 6

This phase occurs at the age of 20.5-20.7 hours. In this period, there is a jump in shrinkage strain. This jump is similar to the drop jump of ettringite. The consequence of this is that development by ettringite also dropped drastically. In this period, apart from CSH and CH, ettringite converts itself into mono sulfate and C(AF)H is formed (Figure 5), as a result, the shrinkage increases drastically. In normal concrete, monosulfate formation occurs in 2 days (Kurtis 2015).

The temperature inside the concrete remains stagnant, or a balance occurs between the release of heat by the formation of hydration products and the absorption of heat by the degradation of ettringite.

So there is no sensitivity of shrinkage strain to heat of hydration.

#### 3.2.1.7. Phenomenon 7

In the range of 20.7-22.7 hours, shrinkage occurred at a low rate, even approaching stagnant. In this period, the formation of all hydration products occurs with a slowdown and ettringite reaches limited amounts, approaching asymptotic levels. Consequently, the temperature inside the concrete remains stagnant.

So there is a sensitivity of shrinkage strain to the heat of hydration.

#### 3.2.1.8. Phenomenon 8

The final phenomenon occurs at the age of 22.7-24 hours. During this period the concrete expands, and the temperature also decreases. However, concerning the concrete expansion time, the temperature decrease is delayed by  $\pm 1$  hour. The number of pores decreases sharply, elongated ettringite needles penetrate the cement core. At this age, the hydration heat flow of cement paste with w/c 0.3 is close to the maximum (Hu *et al.* 2017). This can cause the concrete to expand. Concrete development is not immediately followed by heat release because it is hampered by hydration products which are increasingly mature and increasingly closing the pores (Figure 4).

Thus there is a sensitivity of autogenous deformation to the heat of hydration.

### **4. Conclusion**

The sensitivity of hydration heat to autogenous shrinkage of high-performance concrete beam has been studied. From the research above, it can be concluded that the quality of the mixture is quite good because it can withstand maximum deformation without cracking. During  $\pm 24$  hours the  $C_3A + H + C$  reaction has reached 80%, and the highest heat of hydration comes from  $C_3A$  and then  $C_3S$ . The highest heat occurs at age 9.5-15.5.

The autogenous behavior of HPC within the initial twenty-four hours can be delineated into eight distinct phenomena. Among these, six phenomena exhibit sensitivity to hydration heat. Notably, Phenomenon 3, marked by maximum shrinkage, demonstrates a linear relationship with the heat of hydration. However, two shrinkage strain phenomena, Phenomenon 1 and Phenomenon 6, do not show sensitivity to changes in the heat of hydration. In Phenomenon 1, spanning the first 3 hours post-casting, the concrete temperature is only  $0.5^{\circ}C$  higher than the ambient temperature. Similarly, in Phenomenon 6, characterized by a rapid jump in shrinkage strain, hydration heat remains unaffected.

The eight phenomena occur due to the growth of hydration products and heat release that occurs in the concrete. Based on this, a sketch of the growth of hydration products and changes in the number and size of pores for HPC can be made and is presented in Figure 5.

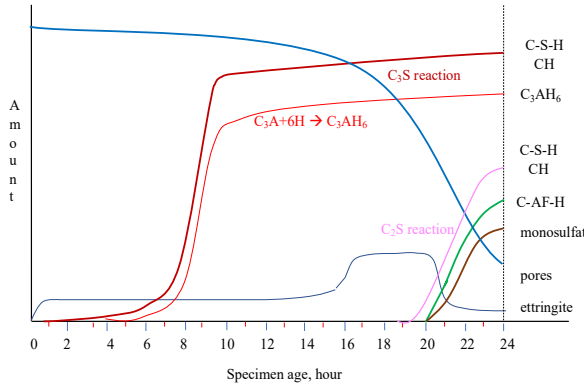


Figure 5. Draft of hydration product and amount of pore growth in HPC

### Acknowledgment

Gratitude is extended to the University of Indonesia, particularly the laboratory led by Mrs. Dr. Elly Tjahjono, for providing essential laboratory resources. Special thanks to the civil engineering department, Faculty of Engineering, University of Lampung for supporting the publication of this paper. Recognition is also due to Mr. Dr. F.X. Supartono for conceptualizing the full-scale concrete beam research and to Mr. Apri for his assistance in installing the vibrating wire-embedded strain gauges (VWESG) and all the Laborans.

### References

1. ACI Committee, ACI 211.4R-93. (1993), "Guide for Selecting Proportions for High-Strength Concrete with Portland Cement and Fly Ash", American Concrete Institute, 13 pages.
2. ACI Committee, ACI 209R-92. (1992), "Prediction of Creep, Shrinkage, and Temperature Effects in Concrete Structure", American Concrete Institute, 1-47.
3. Cai, Y-L., Gao, S-B., Wang, F., Zhang, Z., Zhao, Z., & Ma, B-h. (2023), "Early Hydration Heat Temperature Field of Precast Concrete T-beam under Steam Curin : Experiment and Simulation", *Case Studies in Construction Materials* 18.
4. Chhapola, K. (2023), "Basic Properties of Bouge Compounds C<sub>3</sub>S, C<sub>2</sub>S, C<sub>3</sub>A, C<sub>4</sub>AF", [Online] Available: <https://civilchhapola.com/basic-properties-of-bouge-compounds/>
5. Designing Building, Specific heat: Specific Heat Capacity. [Online] Available: [https://www.designingbuildings.co.uk/wiki/Specific\\_heat\\_capacity](https://www.designingbuildings.co.uk/wiki/Specific_heat_capacity)
6. Hu, X., Shi, C., Shi, Z., Tong, B., Wang, D. (2017), "Early Age Shrinkage and Heat of Hydration of Cement-Fly ash-Slag Ternary Blends", *College of Civil Engineering, Hunan University*, Changsha, Hunan, 410082, PR China, Magnel Laboratory for Concrete Research, Department of Structural Engineering, 7Ghent University, Ghent B-9052, Belgium.
7. Irma, A.H., Nurlita, P., Nur, A.S.T. (2017), "Beton Ramah Lingkungan", Aguscorp, Makasar, Indonesia.
8. Jadhav, S.B. (2021), "Study and Review of Properties & Applications of Low Heat Cement", *International Journal of Regional Planning* 1(1), 15-26.
9. Jia, F., Yao, Y., & Wang, J. (2021), "Influence and Mechanism Research of Hydration Heat Inhibitor on Low-Heat Portland Cement", *Frontiers in Materials* 8.
10. Kim, G., Lee E., & Koo, K. (2009), "Hydration Heat and Autogenous Shrinkage of High-Strength Mass Concrete", *Journal of Asian Architecture and Building Engineering* 8(2), 509-516.
11. Kumar, A., Bishnoi, S., & Scrivener, K.L. (2012), "Modeling Early Age Hydration Kinetics of Alite", *Cement and Concrete Research* 42, 903-918.
12. Kunther, W., Ferreirob, S., & Skibsted, J. (2017), "Influence of the Ca/Si Ratio on the Compressive Strength of Cementitious Calcium–Silicate–Hydrate Binder", *Journal of Material Chemistry* 5, 17401-17412.
13. Kurtis, K. (2015), "Portland Cement Hydration", School of Civil Engineering, Georgia Institute of Technology, Atlanta, Georgia.

14. Lerch, Wm., & Bogue R.H. (1934), "Heat of Hydration of Portland Cement Paste", Part of Bureau of Standards *Journal of Research* **12**, 645-664.
15. Niken, C., Anggita, Y.L., Masdar, H., & Hasti, R.H. (2023), "Autogenous Shrinkage of Normal Concrete Beam with PCC and High-Performance Concrete Beam with OPC", *ULICosTE* Bandar Lampung, Indonesia, September
16. Niken, C., Elly, T., & Supartono, F.X. (2017), "Long-term Deformation of Beam and Column of High-Performance Concrete. *International Journal of Technology* **8** (5), 811-819.
17. Paulini 1992 in Holt, E.E. (2001), "Early Age Autogenous Shrinkage of Concrete", *VTT Publication, Technical Research Centre of Finland* **177** pages.
18. Standar Nasional Indonesia, 15-2049 (2004), "Semen Portland", Badan Standarisasi Nasional, Indonesia
19. Taylor, H.F.W. (1997), "Cement Chemistry", (2<sup>nd</sup> ed.) Thomas Telford, 459 pages, London.
20. Termkhajornkit, P., & Nawa, T. (2006), "A Study of Composition of C-S-H Gel in Cement Paste: Recent Development of Concrete Technology and Structure", *2<sup>nd</sup> ACF International Conference*, November.
21. Wang, J., Hu, Z., Chen, Y., Huang, J., Ma, Y., Zhu, W., Liu, J. (2022), "Effect of Ca/Si and Al/Si on Micromechanical Properties of C(-A)-S-H", *Cement and Concrete Research* **157**.
22. Xu, Y., Ahmad, W., Ahmad, A., Ostrowski, K.A., Dudek, M., Aslam, F., & Joyklad, P. (2021), "Computation of High-Performance Concrete Compressive Strength using Standalone and Ensembled Machine Learning Techniques", *Materials* **14**, 7034.
23. Yalçınkaya, Ç., & Çopuroğlu, O. (2021), "Hydration Heat, Strength and Microstructure Characteristics of UHPC Containing Blast Furnace Slag", *Journal of Building Engineering* **34**.
24. Yogendran, V., Langan, B.W., Haque, M.N., Ward, M.A. (1987), "Silica Fume in High Strength Concrete", *ACI Material Journal* Maret- April.
25. Zhang, T., Wang, H., Luo, Y., Yuan, Y., & Wang, W. (2023), "Hydration Heat Control of Mass Concrete by Pipe Cooling Method and O-Site Monitoring-Based Influence Analysis of Temperature for a Steel Box Arch Bridge Construction", *Materials* **16**(7).
26. Zhao, Y., Li, G., Fan, C., Pang, W., & Wang, Y. (2021), "Effect of Thermal Parameters on Hydration Heat Temperature and Thermal Stress of Mass Concrete", *Advances in Materials Science and Engineering* **2021**.